Hollow cylinder torsional shear tests to evaluate the role of principal stress directions on cyclic resistance

S. Sivathayalan
Carleton University, Ottawa, Ontario, Canada

V. Manmatharajan
Carleton University, Ottawa, Ontario, Canada

P. Logeswaran
EBA Engineering Consultants Ltd, Edmonton, Alberta, Canada

2011 Pan-Am CGS Geotechnical Conference

ABSTRACT
A new hollow cylinder torsional shear device commissioned at Carleton University was used to study the effects of principal stress rotation on cyclic resistance. Specimens at identical initial states were subject to a given cyclic stress ratio, but along stress paths that impose different levels of stress rotation. The paths explored included smooth, continuous rotation of principal stress directions, and sudden jump rotation. These results suggest that the general notion that the weakest response is expected when the major principal stress is aligned with the bedding planes may not be valid under cyclic loading, and cyclic simple shear tests provide a convenient means of determining the cyclic resistance.

RESUMEN
Un nuevo dispositivo tubular para medir esfuerzos de cortante bajo cargas de torsión se ha fabricado en la Universidad de Carleton y ha sido utilizado para estudiar los efectos de la rotación del esfuerzo principal en la resistencia bajo cargas cíclicas. Muestras con condiciones iniciales idénticas fueron sometidas a un esfuerzo cíclico determinado pero siguiendo una trayectoria con niveles diferentes de rotación de esfuerzos. Las trayectorias de carga exploradas incluyen una rotación continua y suave, sin cambios drásticos, y otra con cambios bruscos. Los resultados parecen indicar que, bajo cargas cíclicas, la sigue la dirección de los estratos de depósito en la muestra como se creía. También se demuestra que una prueba cíclica simple de cortante es un ensaye adecuado para determinar la resistencia a cargas cíclicas.

1 INTRODUCTION

Liquefaction susceptibility of soils can be assessed using in-situ test and empirical correlations, or from laboratory tests. It is not uncommon to use a combination of both laboratory and in-situ methods in projects of significance. Laboratory assessment should preferably be conducted on undisturbed specimens consolidated to in-situ stress states, and subjected to anticipated field loading paths. However, geometry and configuration of laboratory testing devices limit the possible consolidation stress states, and stress paths. Most natural soils are inherently anisotropic, and their response has been shown to be dependent on loading direction (Vaid et al. 1990a).

The triaxial test is probably the most commonly used geotechnical test to assess the mechanical behaviour of soils. Triaxial devices have become the choice for routine soil testing due to their simpler design, and straightforward testing procedures. Principal stress directions are fixed in the vertical and horizontal planes in a triaxial test, and two of the principal stresses are always equal on account of the axisymmetry. Triaxial tests are often conducted on hydrostatically consolidated specimens, and infrequently on specimens consolidated to different vertical and horizontal stresses.

Soils deposited naturally under gravity tend to have a horizontal bedding plane, and exhibit much stronger response under triaxial compression loading, where major principal stress, σ_1 acts vertically, compared to triaxial extension mode of loading, where σ_1 acts horizontally. The effect of the intermediate principal stress is comparatively smaller, and is often assessed using the parameter $b = (\sigma_2 - \sigma_3)/(\sigma_1 - \sigma_3)$, which is zero in triaxial compression, and one in triaxial extension. Initial shear in a hydrostatically consolidated triaxial specimens is zero ($\tau_{st} = 0$), but initial (static) shear stresses in specimens consolidated to a non-hydrostatic initial state is equal to $\tau_{st} = (\sigma_{1c} - \sigma_{3c})/2$, where σ_{1c} and σ_{3c} are the major and minor principal stresses at the end of consolidation respectively. Typically major principal stress acts along the deposition direction, and hence $\sigma_{1c} = \sigma_{vc}$.

A cyclic triaxial test is typically conducted by applying a cyclic axial load to simulate seismic loading while keeping the cell pressure constant. Intensity of cyclic shaking is quantified by the cyclic stress ratio, CSR which is commonly derived by normalising the peak cyclic stress

τ_{cy} (or half the cyclic deviator stress, $\sigma_{d,cy}$) by the confining pressure σ_{3c} to yield $CSR = (\sigma_{1c} - \sigma_{3c})/2\sigma_{3c}$. Vaid et al. (2001) noted that a modified definition given by $CSR = (\sigma_{1c} - \sigma_{3c})/(\sigma_{1c} + \sigma_{3c})$ would provide a consistent basis for comparing CSR values between triaxial and simple shear tests. Depending on the relative magnitudes of initial shear stress τ_{st} and cyclic shear stress τ_{cy}, principal stress direction could remain fixed throughout the loading (if $\tau_{st} > \tau_{cy}$), or suddenly jump by 90° (when $\tau_{st} < \tau_{cy}$) in a cyclic triaxial test. The peak shear stresses are always applied on planes inclined at $45°$ to vertical regardless of the initial static shear. A schematic illustration of the stress states in a triaxial test are shown in Figure 1.

A cyclic simple shear test is conducted by applying the cyclic shear stress τ_{cy} on the horizontal plane under plane strain loading conditions. Simple shear devices enable appropriate simulation of in-situ stress states during consolidation. Level ground conditions are represented by K_o consolidation, and stress states on sloping ground, such as embankments and dams, can be simulated by adding a shear stress on the horizontal plane during consolidation. Major and minor principal stresses rotate during cyclic simple shear loading, typically between $\pm 45°$. These rotations cannot be controlled, and the orientation of the major principal stress cannot exceed $45°$ to vertical. In other words, the major principal stress is never aligned along the along the weakest (horizontal) plane.

A simple shear device (Bjerrum & Landva, 1966) is recognized to simulate the stress conditions in-situ due to vertically propagating shear waves well, since the cyclic shear stress is applied on the horizontal plane, and principal stresses rotate continuously during the loading. The outcome of such similitude is that cyclic resistance measured from simple shear tests closely represents the in-situ capacity of the soils. Cyclic resistance measured in triaxial tests cannot be directly applied to in-situ soils due to the stress path effects, and a correction factor, C_r (Peacock & Seed, 1971; Vaid & Sivathayalan, 1996) is used convert the triaxial resistance to simple shear resistance.

2 STRESS PATH DEPENDENT BEHAVIOUR

Stress state and path dependent behaviour of sands has been demonstrated by several researchers (Vaid & Chern, 1985; Vaid et al. 1990; Vaid & Sivathayalan, 1996; Uthayakumar & Vaid, 1998; Yoshimine et al. 1999). Water deposited sands have been shown to strain harden even at the loosest deposited state in triaxial compression (Vaid & Thomas, 1995). However, they strain soften over a range of density states under triaxial extension loading. The direction of the major principal stress, α_σ with respect to the deposition direction is responsible for such dramatic differences in the behaviour. Figure 2 shows the behaviour of sand consolidated to identical initial stress and density states and sheared along different orientations of major principal stress under plane strain conditions. A systematic softening of the response occurs as α_σ increases and the major principal stress aligns towards the bedding planes.

Figure 3 compares the undrained response of Toyura sand at similar initial states, but under different loading modes. The sand strain hardens under triaxial compression ($\alpha_\sigma = 0, b = 0$), and only marginally strain softens under simple shear ($\alpha_\sigma \approx 45°, b \approx 0.4$), but it undergoes significant strain softening in triaxial extension ($\alpha_\sigma = 90°, b = 1$). The strength mobilised in extension loading in only a fraction of that mobilised in simple shear. Figures 2 and 3 clearly demonstrate that the weakest response under monotonic loading manifests when the direction of the major principal stress aligns with the bedding planes.

Soil element in-situ could be subjected to different

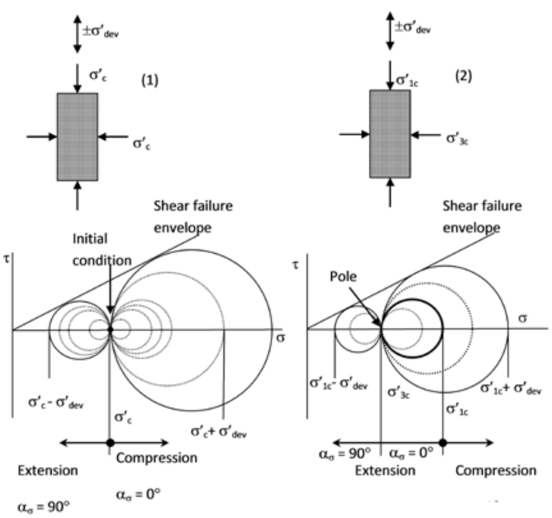

Figure 1. Stress states in a triaxial specimen depending on the initial consolidation stress state

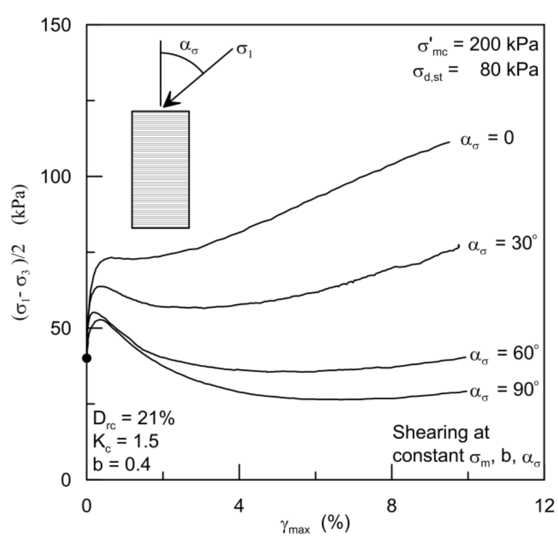

Figure 2. Influence of principal stress direction on the monotonic undrained response of sands (after Sivathayalan & Vaid, 2002)

types of cyclic loading, depending on the type of waves (p-wave, s-wave, or surface waves) and the direction of wave propagation. The magnitudes of the horizontal and vertical acceleration components are indicative of the nature of the loading. It is common practice to use simpler models of seismic shaking to evaluate the response of soils, and the most widely used 'SHAKE' (or similar) analysis model the response due to a vertically propagating shear wave. While this might be a good approximation in many cases, the true nature of the loading would depend on the type of the wave, inclination of bedrock, and impedance contrast $(\rho_1 v_1/\rho_2 v_2)$ between bedrock and overlying soil, and local site effects. Even in the simpler case of vertically propagating waves, interactions of s-waves and p-waves could lead to a more generalized loading that involves principal stress rotation through larger angles. Even though p-waves, and s-waves arrive at a site at different times, local site effects including wave reflections at bedrock can lead to such loading. This is especially the case when the impedance contrast between the bedrock and soils is fairly large. Further, the surface waves, and specifically the Rayleigh waves which consist of both dilatational and shear components could lead to such generalised loading.

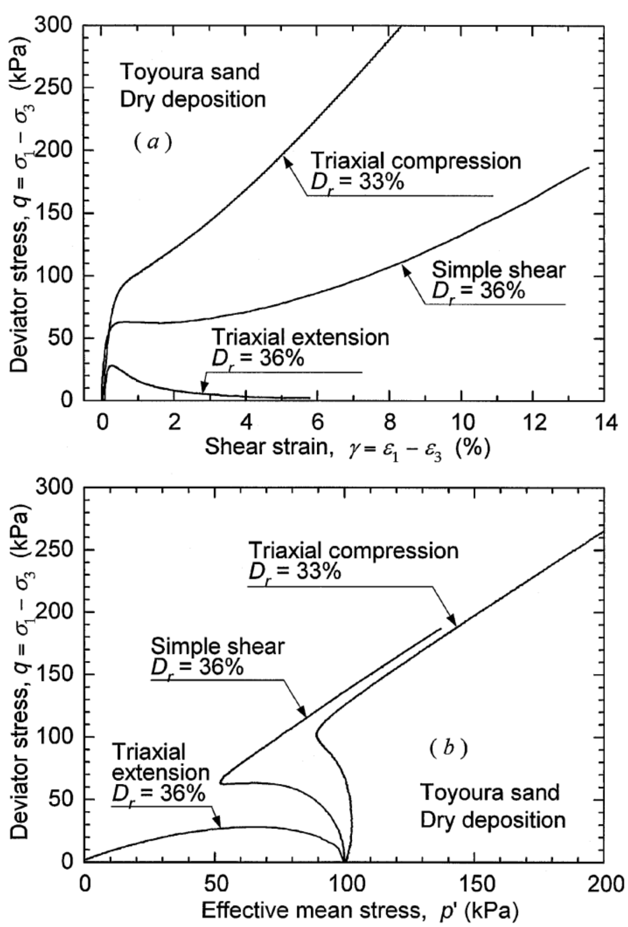

Figure 3. Influence of loading mode on the monotonic undrained response of sands (after Yoshimine et al. 1999)

The possible in-situ loading modes, combined with the data presented in Figures 2 & 3 raise a concern about the use of cyclic simple shear tests to characterize earthquake response. While a simple shear device simulates the in-situ loading under vertically propagating shear waves (and thus principal stress rotation of up to $\pm 45°$) it is not capable of simulating in-situ loading that might involve larger rotation of principal stresses. If the weakest cyclic response follows the same patterns noted in monotonic loading then relying on cyclic simple shear data might potentially lead to unsafe designs. The objective of this research program is to estimate the effects of different levels of stress rotation on cyclic resistance of soils, and assess whether such a risk exists.

3 HOLLOW CYLINDER TORSIONAL SHEAR TEST

Hollow cylinder torsional shear device is a versatile apparatus for measuring the mechanical behaviour of soils under generalized loading. The general outlook of this device is similar to a traditional triaxial test, but the specimen is an annular ring, and thus permits application of internal pressure and torque (to control the shear stress on the horizontal plane), in addition to external cell pressure and vertical load. These variables can be independently controlled, and thus this test permits independent control of the three principal stresses $\sigma_1, \sigma_2 \,\&\, \sigma_3$ and the inclination α_σ of σ_1, σ_3 in one plane. Traditional triaxial and simple shear tests can only control two independent parameters $(\sigma_1 \; and \; \sigma_3)$ compared to the four in HCT tests.

Shear stresses induced on account of torsion vary with radius, and thus hollow cylinder specimens typically use relatively thin walls (10-20% of the diameter) to minimize shear stress non-uniformities. In addition, differences between the internal (P_i) and external (P_e) pressures lead to a stress gradient across the wall. These pressures depend on prescribed test parameters, and are generally kept closer to each other to minimize the stress non-uniformities. Significant research efforts over the years have identified suitable sizing to minimize the stress non-uniformities (Sayao, 1989; Wijewickreme, 1990). The use of hollow cylindrical specimens have been proposed decades years ago, but their use in undrained liquefaction studies involving complex stress paths has become feasible with the advent of high-speed, high resolution data acquisition and control systems (Symes et al. 1985; Uthayakumar 1996; Uthayakumar & Vaid, 1998; Logeswaran, 2010)

3.1 CU HCT Device

The HCT device at Carleton University system was custom built by AllpaTech Geotechnical Instruments Inc. of Richmond, BC. This device uses a specimen with an outer diameter of 150 mm, inner diameter of 100 mm and a height of 300 mm. These dimensions are chosen to minimize the stress non-uniformities across the wall under typical test conditions. This device is equipped with high speed (333 kS/s) and high resolution data acquisition system connected to state of the art Electro-Pneumatic Transducers (EPT), Stepper Motor Drives (SMD), and

Figure 4. Hollow cylinder torsional shear device at Carleton University

high precision transducers to enable confident and repeatable measurements of loads, volume changes and displacements. Three EPTs enable computerised control of inner pressure, outer pressure and vertical load. A pair of torque motors are used to apply torsional displacements, and torsional shear stress targets are reached using a feedback loop.

A total of nine transducers are used to measure the stress and strain components. Inner (P_i) , outer (P_e) and pore pressure are measured using pressure transducers with a resolution of 0.05kPa. The vertical load (F_z) and torque (T_h) are measured by a combined thrust-torque cell with a resolution of approximately 0.1Nm for torque measurements (shear stress in the order of 0.2kPa) and approximately 1N for axial load measurements (vertical stress in the order of 0.1kPa). Changes in the inner (R_e) and outer (R_i) radii of the specimen are estimated from the measured volume changes of the inner cavity and the sample. Average vertical (σ_z), radial (σ_r) tangential (σ_θ) and torsional shear $(\tau_{z\theta})$ stresses in the sample were calculated using force equilibrium considerations as shown in eq. 1 (Vaid et al. 1990b).

$$
\begin{aligned}
\sigma_z &= \frac{F_z + \pi\left(P_e.R_e^2 - P_i.R_i^2\right)}{\pi\left(R_e^2 - R_i^2\right)} \\
\sigma_r &= \frac{\left(P_e.R_e^2 - P_i.R_i^2\right)}{\left(R_e^2 - R_i^2\right)} + \frac{2(P_e - P_i)\,R_e^2\,R_i^2 \ln(\mathrm{R_e}/\mathrm{R_i})}{\left(R_e^2 - R_i^2\right)^2} \\
\sigma_\theta &= \frac{\left(P_e.R_e^2 - P_i.R_i^2\right)}{\left(R_e^2 - R_i^2\right)} - \frac{2(P_e - P_i)\,R_e^2\,R_i^2\, ln\,(R_e/R_i)}{\left(R_e^2 - R_i^2\right)^2} \\
\tau_{z\theta} &= \frac{4\,T_h\left(R_e^3 - R_i^3\right)}{3\pi\left(R_e^4 - R_i^4\right)\left(R_e^2 - R_i^2\right)}
\end{aligned}
\tag{1}
$$

Axial strain (ε_z) is determined directly from the measured vertical displacement $(\varepsilon_z = \Delta H/H)$, and the average radial (ε_r) tangential (ε_θ) and torsional shear $(\gamma_{z\theta})$ strains are calculated using the following set of equations.

$$
\begin{aligned}
\varepsilon_r &= (\Delta R_e - \Delta R_i)/(R_e - R_i) \\
\varepsilon_\theta &= -\,(\Delta R_e + \Delta R_i)/(R_e + R_i) \\
\gamma_{z\theta} &= \frac{2.\Delta\theta.\left(R_e^3 - R_i^3\right)}{3\,H\left(R_e^2 - R_i^2\right)}
\end{aligned}
\tag{2}
$$

The principal stresses and strains are determined from these components. During cyclic loading, the required cyclic deviator stress is calculated at each time step (depending on CSR), and the required surface tractions are computed given the constraints (e.g., principal stress directions).

A multithreaded data acquisition program was developed in-house to acquire the data, and control the system. Multiple execution threads to scan transducer readings, save the data to a file, control EPTs and SMDs (one thread per each SMD, and one for EPTs) within a single process enable continuous and smooth operation of the control hardware, and proper sampling of the input channels without interruption or delay. This enabled overcoming a bottleneck encountered in traditional data acquisition programs that utilize the internal system clock of the personal computer. Such data acquisition programs are generally limited to using only one CPU, and have a limited timer resolution of about 55ms, which is not adequate for feedback controlled loading.

3.2 Test material

Cyclic shear tests were carried out on sand dredged from the Fraser River near Abbotsford, British Columbia. The original sand was wet-sieved through #200 sieve to remove the fine particles (less than 5%) and then dry-sieved thorough #20 sieve to remove the coarse particles (less than 1%). The removal of coarse and fine material yields fairly uniform sand with mean diameter of 0.30 mm, and a uniformity coefficient of 2.9. Such uniform material facilitates fundamental laboratory studies that require several repeatable, homogeneous specimens. The Fraser Delta sand has been used in several past studies and reported in the literature (Vaid & Thomas, 1994; Sivathayalan & Vaid, 2002; Logeswaran & Sivathayalan 2005). The maximum and minimum void ratios of this batch of Fraser Delta sand determined according to the ASTM test standards (ASTM D4253, D4254) are 0.806 and 0.509.

3.3 Specimen preparation technique

Undrained response of sands, and thus liquefaction potential are highly dependent on the soil fabric that ensues during the natural deposition process in-situ (Vaid et al. 1999). Different reconstitution methods result in different fabric. The method of reconstitution used in the laboratory should simulate the natural deposition process, if laboratory results are to be applied to in-situ soils with confidence. Specimens were reconstituted by water pluviation (Vaid & Negussey, 1988) to simulate the natural deposition process of alluvial/fluvial soil deposits. Vaid et al. (1999) noted that the mechanical response of water pluviated specimens is similar to that of undisturbed fluvial sands. In addition, high repeatability of this specimen preparation technique permits the reconstitution of several identical specimens, which is an essential requirement in fundamental experimental studies.

4 CYCLIC STRESS-ROTATION TESTS

4.1 Test Program

A series of cyclic tests were conducted on the loosest deposited Fraser River sand consolidated to a hydrostatic effective stress state of 200 kPa. The relative density following consolidation was about 22%. Both the total mean normal stress (400 kPa), and the intermediate principal stress parameter (b = 0) were maintained constant during cyclic shearing. A sinusoidal cyclic deviator stress, with a peak $\sigma_{d,cy} = 60\ kPa$ was applied in all tests to yield a constant CSR = 0.15. The orientation of the major principal stress was changed smoothly with the deviator stress as shown in Figure 5. The maximum rotation, which corresponds to the inclination of the major principal stress at the instant of peak shear stress, $\alpha_{\sigma,max}$ was varied between $30°$ and $90°$ as shown in Table 1.

Table 1. Test Parameters

Test	Consolidation state	Cyclic loading	
		$\alpha_{\sigma,max}$	$\sigma_{d,cy}/2\sigma_{vc}$
1		$30°$	
2	σ'_{mc} = 200 kPa	$45°$	
3	K_c = 1	$60°$	0.15
4	D_r =21.7 $\pm$ 0.3%	$75°$	
5		$90°$	
6		$30°$	0.20
7		$30°$	0.25

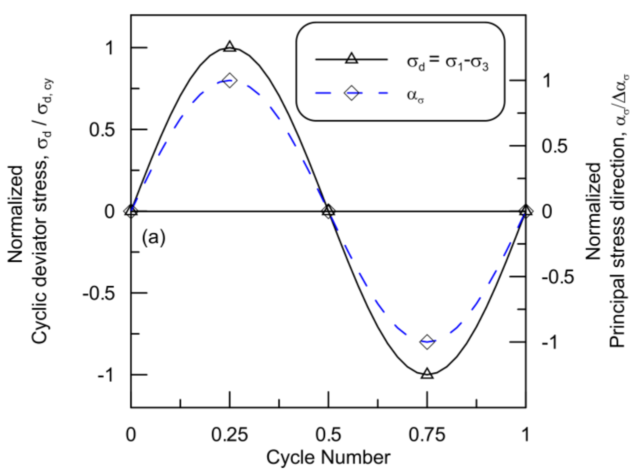

Figure 5. Variation of deviator stress, and imposed principal stress direction during cyclic loading

Cyclic loading was applied at a fairly long period of four minutes per cycle. Such a slow rate was required because of the feedback control loop used to target the torsional shear stresses. The feedback control loop caused minor oscillations ('noise') in the measurements compared to tests without feedback control, but these oscillations were fairly small, and within acceptable range. The imposed paths correspond to symmetric stress rotation about the vertical axis between $\pm\alpha_{\sigma,max}$, and thus the principal stresses rotate through an angle of $2\alpha_{\sigma,max}$ in each test. Uthayakumar (1998) conducted similar cyclic stress rotation tests to assess the effects of aligning the major principal stress along the bedding planes during cyclic loading. Principal stresses rotation was limited to $90°$ in that study. Specimens were deemed to have liquefied when the maximum shear strain exceeded 3.75% (NRC 1985). Cyclic stress ratio CSR in hollow cylinder tests is normally defined by normalising the peak cyclic shear stress τ_{cy} $\left(= \sigma_{d,cy}/2\right)$ by the effective mean normal stress, σ'_{mc}. In hydrostatically consolidated specimens, vertical consolidation stress σ_{vc} can be used as a substitute for σ_{mc}, and hence $CSR = \sigma_{d,cy}/2\sigma_{vc}$.

4.2 Test Results & Discussion

Figure 6 shows the cyclic undrained behaviour of Fraser River sand subjected to smooth rotation of principal stresses between $+45^o$ and -45^o at a cyclic

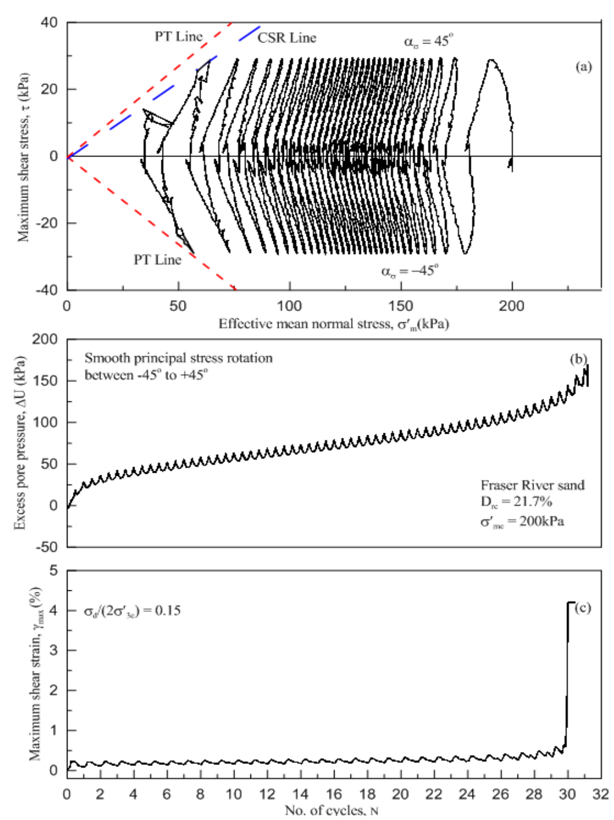

Figure 6. Cyclic behaviour of Fraser Delta sand subjected to a smooth rotation of principal stress between $+45^o$ and -45^o at stress ratio of 0.15

stress ratio of 0.15. The direction of the principal stresses linearly varied with the cyclic shear stress at every instant, and the maximum inclinations were reached when the peak shear stress state was applied. Unlike the effective stress paths in cyclic triaxial tests which show significant non-symmetry in the cyclic stress path, the effective stress path in this case can be noted to be fairly symmetric (except at the extreme stages of the loading). One cannot expect perfect symmetry since the effective stresses are changing during the loading, but changes within each half-cycle are fairly small and hence reasonable symmetry is noted in the stress path. Such symmetry is reflective of the existence of an isotropic fabric in the horizontal direction. The effective stress path gradually moves toward the origin, and strain development was fairly small until the sand suddenly develops large strain during the 30^{th} cycle. Such sudden strain development is characteristics of true and limited liquefaction type of response. The maximum excess pore pressure generated due to liquefaction was about 160 kPa, which is equivalent to about 80% of the initial effective confining stress.

Figure 7 shows the dependence of the number of cycles to liquefaction at different CSR values for a constant level of principal stress rotation ($\alpha_{\sigma,max} = 30°$). Corresponding test numbers given in Table 1 are noted in the figure next to the data points for clarity. Orientation of the major principal stress increased to $+30°$ during the first quarter cycle of the cyclic loading, and then decreased to $-30°$ during the next half cycle as illustrated in Figure 5. The number of cycles to liquefaction decreased from 118 cycles at CSR = 0.15 to 14 cycles at CSR = 0.2, and to 5 cycles at CSR = 0.25. The rate of reduction noted is fairly consistent with the experience derived from cyclic simple shear and cyclic triaxial tests.

Figure 8 shows the variation of the number of cycles to liquefaction as a function of the degree of stress rotation. As noted in Table 1, the initial states of the specimen are essentially identical, and the specimens were subjected to a fixed CSR = 0.15. The drastic differences in the number of cycles to liquefaction clearly highlight the influence of stress rotation. Increasing degree of stress rotation decreases the cyclic resistance up to a certain level, but the cyclic resistance increases afterwards. Essentially similar resistance was noted at 45^o and 60^o stress rotation angles. The reduction in cyclic resistance with increasing stress rotation was anticipated, and consistent with the expectations. However, the fairly significant increase in resistance at large levels of stress rotation appears to be counter intuitive. It is clearly contrary to the current understanding that progressively weaker responses are to be expected as the major principal stress aligns toward the weaker horizontal direction.

The major principal stress aligns with the weakest horizontal (bedding plane) direction in test #5 (with 90^o stress rotation) twice during each cycle, when the peak cyclic shear stress of 30 kPa is applied during cyclic loading. Comparatively, the inclination of the major principal stress at the instant of the peak cyclic shear stress is only half that (i.e., $45°$) in test #2. Yet, test #5 requires three times as many cycles to liquefy compared to test #2. These findings appear to contradict the observations noted under monotonic loading where alignment of the major principal stress toward the bedding plane always led to softer response (Figures 2, 3).

It appears that the inclination of the plane of peak shear stress with respect to the bedding plane, and the magnitude of the shear stress on the weak horizontal (bedding) plane are probably responsible for the observed behaviour. Even though all tests were conducted at the same CSR of 0.15, (which yields a constant peak cyclic shear stress of 30 kPa), the shear stress on the horizontal plane ($\tau_{z\theta}$) varied among tests. The variation of cyclic

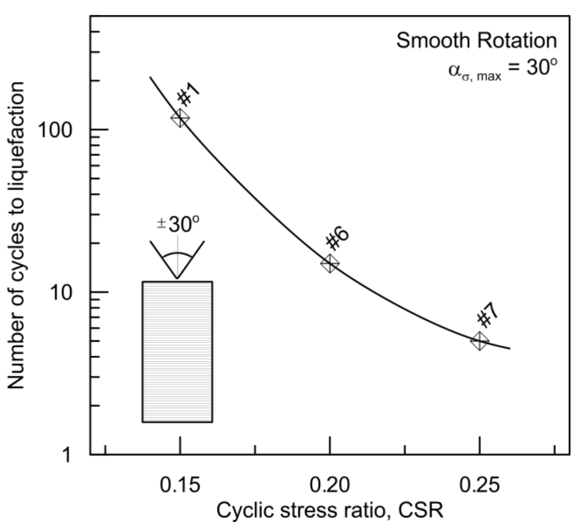

Figure 7. Variation of the number of cycles to liquefaction with cyclic stress ratio in specimens subjected to $\pm 30°$ principal stress rotation about the vertical axis.

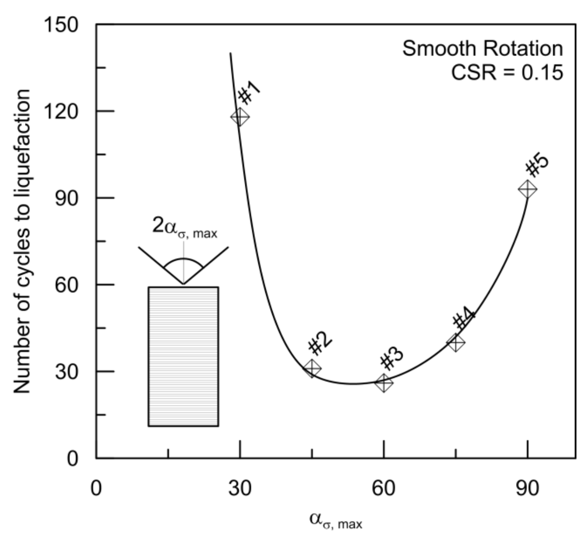

Figure 8. Variation of the number of cycles to liquefaction with $\alpha_{\sigma,max}$ in specimens subjected to CSR = 0.15.

deviator stress, principal stress direction α_σ, and $\tau_{z\theta}$ with time are given by

$$\sigma_d = 2\,.\,CSR.\,\sigma'_{vc}\,.\sin[2\pi t/T]$$

$$\alpha_\sigma = \alpha_{\sigma,max}\,.\sin[2\pi t/T] \qquad (3)$$

$$\tau_{z\theta} = CSR\,.\,\sigma'_{vc}.\left|\sin\left(2.\,\alpha_{\sigma,max}\,.\sin\left[\frac{2\pi t}{T}\right]\right)\right|.\sin\left[\frac{2\pi t}{T}\right]$$

The peak value of $\tau_{z\theta}$ is obviously dependent on the magnitude of stress rotation $\alpha_{\sigma,max}$. The variation of the shear stress on the horizontal plane during one cycle in tests with different levels of stress rotation, but the same CSR is shown in Figure 9. The shear stress on the horizontal plane attains a maximum value of 30 kPa in the test with $\alpha_{\sigma,max} = 45°$, but the maximum value of shear stress on the horizontal plane in the $\alpha_{\sigma,max} = 90°$ test is only about 17 kPa. In addition, the peak value occurs when the major principal stress is inclined at an angle of about $\alpha_\sigma = 36°$, and the shear stress on the horizontal plane when $\alpha_\sigma = 90°$ is zero. These observations provide an explanation for the observed, apparently contradictory, behaviour.

5 SUMMARY & CONCLUSIONS

An experimental research program was undertaken to better understand the influence of principal stress rotation on cyclic resistance. This is intended to represent field loading conditions where elements are subjected to simultaneous cyclic loading in the vertical and horizontal planes. Preliminary results of the research program presented here indicate that the notion that progressively weaker responses are to be expected as the major principal stress aligns toward the weaker horizontal direction is always valid.

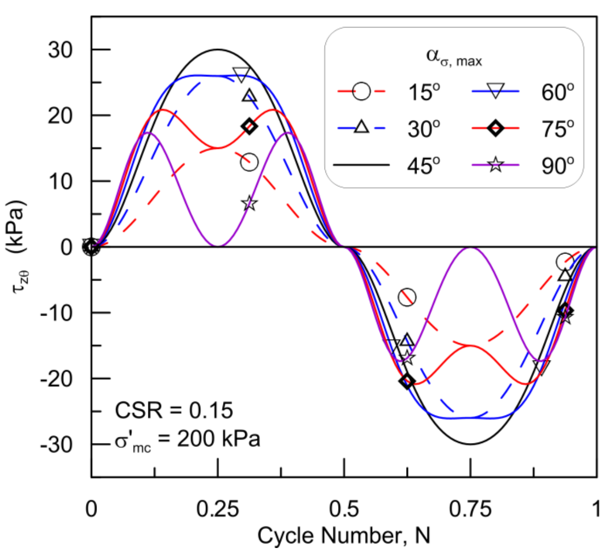

Figure 9. Variation of the shear stress on the horizontal plane during the loading cycle.

Principal stress directions were changed smoothly during cyclic loading by prescribed magnitudes. Axial symmetry was maintained, and rotation angles varied from 30° to 90° about the deposition direction. These test results suggest that strength anisotropy is not only dependent on the direction of the major principal stress with respect to the bedding planes, but it also depends on the inclination of the plane of peak shear stress to the bedding plane. Such a hypothesis, explains why the lowest cyclic resistance was measured in tests with principal stress rotation of about $\pm 45°$ to $\pm 60°$. These results suggest that cyclic simple shear tests will not lead to unsafe designs on account of the limited stress rotation in simple shear.

ACKNOWLEDGEMENTS

The writers would like to acknowledge the financial support provided through the Discovery Grants program of the Natural Sciences and Engineering Research Council. The equipment grants awarded by the Canada Foundation for Innovation and Ontario Innovation Trust were instrumental in establishing the experimental infrastructure used for this research. Technical assistance of Stan, Pierre, Jason and Jim has been invaluable in maintaining the laboratory equipment, and is gratefully acknowledged. Authors very much appreciate, and acknowledge the help of Prof. Juan Salinas in translating the abstract.

REFERENCES

ASTM D4253. 2000. Standard test methods for maximum index density and unit weight of soils using a vibratory table. ASTM International.

ASTM D4254. 2000. Standard test methods for minimum index density and unit weight of soils and calculation of relative density. ASTM International.

Bjerrum, L. and Landva, A., 1966, Direct simple-shear tests on a Norwegian quick clay, *Geotechnique*, 16(1): 1-20..

Logeswaran, P., 2010, Behaviour of sands under generalized loading and drainage conditions, PhD Thesis, *Carleton University*, 274p.

Logeswaran, P., and Sivathayalan, S., (2005), Characterization of response of Fraser River sand under simultaneous changes in volume and pore pressure, *58th Canadian Geotechnical Conference,* Saskatoon, Saskatchewan, Canada, Sept. 19 - 21, 2005

Peacock, W. H. and Seed, H. B., 1968, Sand liquefaction under cyclic loading simple shear conditions, *ASCE Journal of the Soil Mechanics and Foundation Engineering Division*, 94(SM3): 689-708.

Sayao, A.S.F., 1989, Behaviour of sand under generalised stress paths in the hollow cylinder torsional device, PhD Thesis, *University of British Columbia*, Vancouver, Canada, 196p.

Sivathayalan, S. & Vaid, Y. P., 2002, Influence of generalized initial state and principal stress rotation on the undrained response of sands, *Canadian Geotechnical Journal*, 39(1): 63-76

Symes, M.J.P.R., Shibuya, S., Hight, D.W. & Gens, A, 1985, Liquefaction with cyclic principal stress rotation, *In Proc. of the Eleventh International Conference on Soil Mechanics and Foundation*, San Francisco, 11(4): 1919-1922.

Vaid, Y.P. & Chern, J.C., 1985, Cyclic and monotonic undrained response of saturated sands, *In Proc. of Advances in Testing Soils under cyclic conditions*, Ed. Khosla, V., Detroit, MI., pp. 120-147.

Vaid, Y.P., Chung, E.K.F., and Kuerbis, R.H., 1990a, "Stress Path and Steady State", *Canadian Geotechnical Journal*, Vol. 27(1), pp. 1-7.

Vaid, Y.P., Sayao, A., Enhuang, H. and Negussey, D., 1990b, Generalized Stress-Path Dependent Soil Behaviour with a New Hollow Cylinder Torsional Apparatus, *Canadian Geotechnical Journal*, Vol. 27(5), pp. 601-616.

Vaid, Y. P. and Negussey, D., 1988, "Preparation of reconstituted sand specimens", *Advanced Triaxail Testing of Soils and Rock, ASTM Special Technical Publication 977*, Eds: Donaghe, R. T., Chaney, R. C., and Silver, M. L., Philadelphia, pp. 405-417.

Vaid, Y.P. & Sivathayalan, S, 1996. Static and cyclic liquefaction potential of Fraser Delta sand in simple shear and triaxial tests, *Canadian Geotechnical Journal*, 33(2): 281-289.

Vaid, Y.P. & Sivathayalan, S, 2000, Fundamental factors affecting liquefaction susceptibility of sands, *Canadian Geotechnical Journal*, 37(3): 592-606

Vaid, Y.P. & Thomas, J, 1995, Liquefaction and post liquefaction behaviour of sand, *ASCE Journal of Geotechnical Engineering*, 121(2): 163-173.

Vaid, Y.P., Sivathayalan S., & Stedman D, 1999, Influence of specimen-reconstituting method on the undrained response of sand, *Geotechnical Testing Journal*, 22(3): 187-196

Vaid, Y. P., Chung, E. K. F., and Kuerbis, R. H., 1990, Stress path and steady state, *Canadian Geotechnical Journal*, 27(1): 1-7

Uthayakumar, M., 1996, Liquefaction of sands under multiaxial loading, PhD Thesis, *University of British Columbia*, Vancouver, Canada, 198p.

Uthayakumar, M. and Vaid, Y. P., 1998, Static liquefaction of sands under multiaxial loading, *Canadian Geotechnical Journal*, Vol. 35, No. 2, pp. 273-283.

Wijewickreme, W. K. D., 1990, Behaviour of sand under simultaneous increase in stress ratio and principal stress rotation, PhD Thesis, *University of British Columbia*, Vancouver, Canada, 225p.

Yoshimine, M., Robertson, P. K., & Wride, C.E., 1999, Undrained shear strength of clean sands to trigger flow liquefaction, *Canadian Geotechnical Journal*, 36(5): 891-906